Supplementary Discussion for 'Cooperative protofilament switching emerges from inter-motor interference in multiple-motor transport'

David Ando, Michelle K. Mattson, Jing Xu, and Ajay Gopinathan

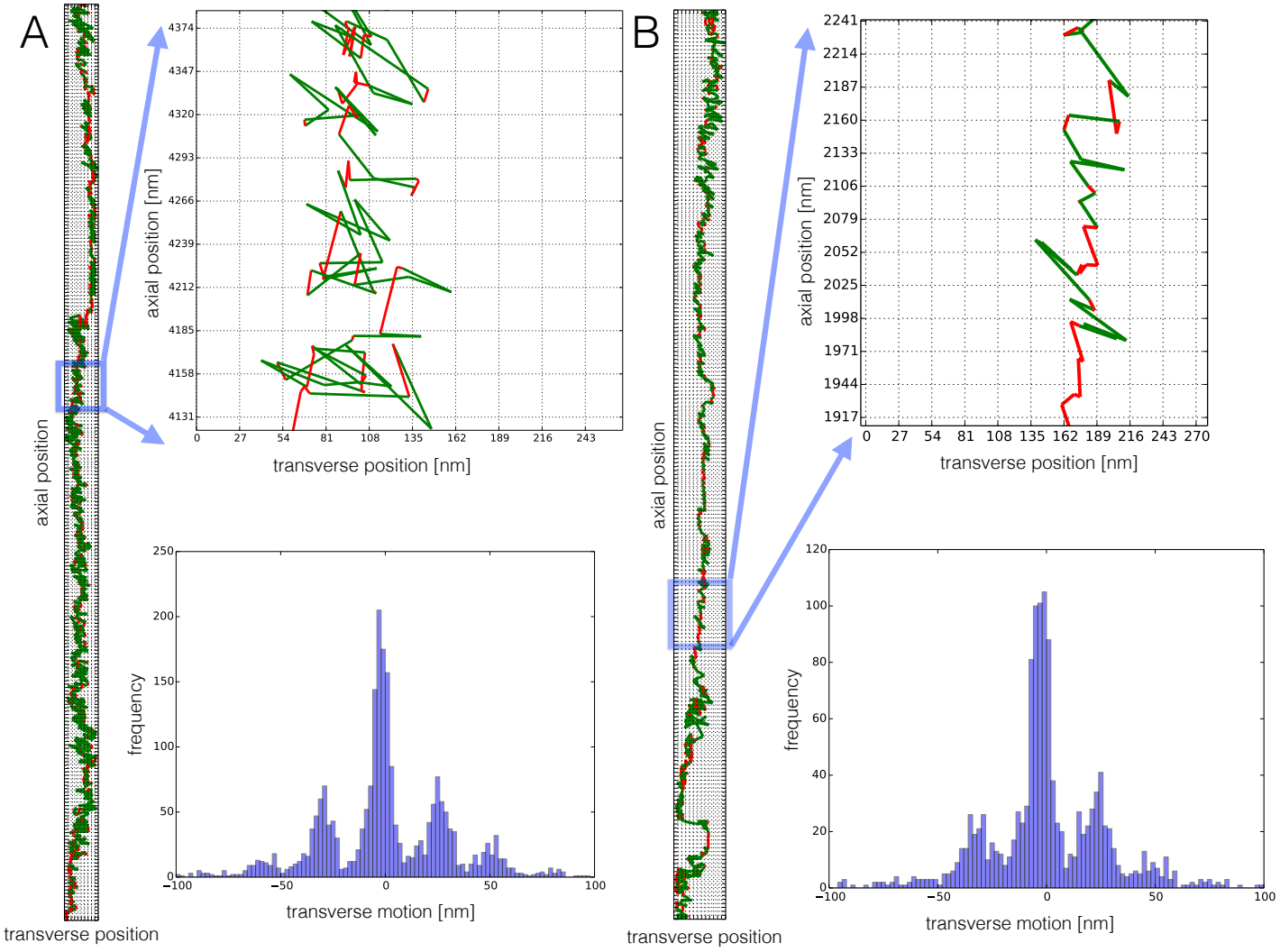

Supplementary Fig. 1: Representative traces of cargo position for two kinesin motors at 10 μM ATP for two sample traces (A) and (B). For visualization of the DTD events in these traces, frames which are likely DTD events (transverse displacement greater than 13.5 nm, Figure 1B) have been colored green while likely non-DTD event containing frames are colored red in 2D plots of these two representative traces. Histograms of the magnitude of transverse motion for each sample trace are shown in blue.

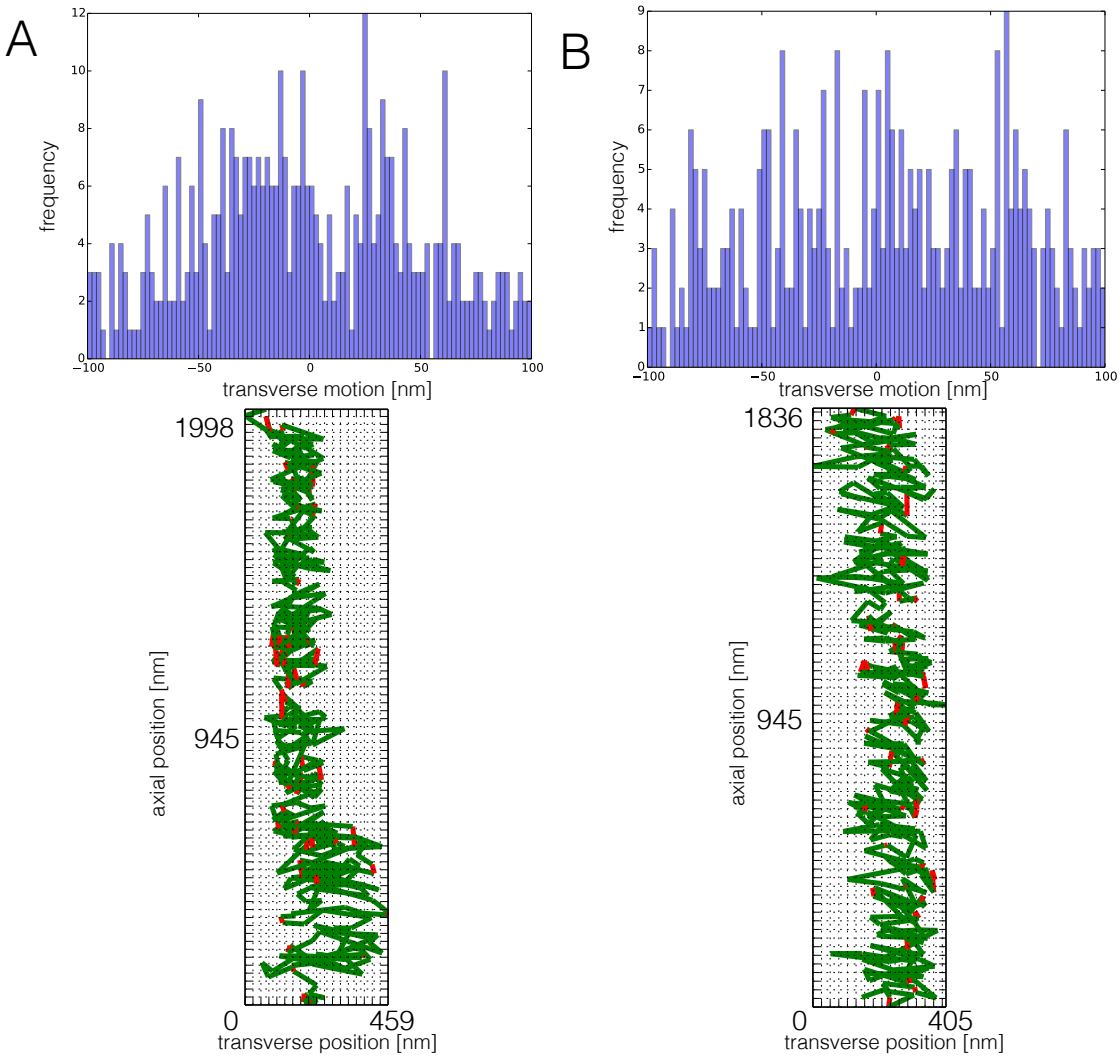

Supplementary Fig. 2: Representative traces of cargo position for single kinesin motors at 10 μM ATP for two sample traces (A) and (B). For visualization of the transverse motion during frames in these traces and comparison to DTD events in two motor traces, frames which have a transverse displacement greater than 13.5 nm have been colored green while those with a small transverse displacement are colored red in 2D plots of these two representative traces. Histograms of the magnitude of transverse motion for each sample trace are shown in blue.

1 Motor-cargo displacement

Assuming a rigid kinesin-bead complex, where motors are perpendicular to the microtubule surface, the change in measured transverse position of a bead's center of mass can be related to the change in the center of mass of the kinesin motor heads along the microtubule surface by a geometrical projection of the following form (Supplementary Fig. 1):

$$\delta CM_{heads} = \delta CM_{bead}(\frac{L_h}{R_{bead} + L_h + L_{kinesin}}) \tag{1}$$

With variables R_{bead} = bead radius, $L_{kinesin}$ = length of kinesin motors (measured from attachment to bead to CM of motor heads), and L_h = distance from center of microtubule to kinesin motor head's center of mass.

The size of DTD events, which are measured relative to the change in center of mass of the transported *bead*, is constant within a given trace at around 27 nm in the transverse direction and different traces consistently show this same magnitude for DTD events. Within experimental uncertainties for bead size, kinesin motor length, and microtubule geometry, we calculate that DTD events with a 27 nm transverse displacement correspond to a 1.4 nm shift in the center of mass of the kinesin motor *heads*:

$$\delta CM_{heads} = 27 \pm 2nm(\frac{15 \pm 1.0nm}{220 \pm 20nm + 15 \pm 1.0nm + 60 \pm 20nm}) \sim 1.4 \pm 0.4nm \tag{2}$$

For a 13 protofilament microtubule, a sidestep for an individual kinesin motor head involves a 5.6 nm movement in the transverse direction given the structure of the microtubule binding regions (Fig. 2A). The movement of a single kinesin head (among 4 present in our double motor construct) to an adjacent microtubule protofilament would therefore result in the center of mass of all motor heads changing by 1.4 nm, i.e. 5.6 nm / 4 = 1.4 nm (as long as motors a roughly localized to the same region of the microtubule). We can therefore conclude that the motion of a motor head moving to an adjacent protofilament imposes a magnitude of transverse motion to the transported bead equal in size to DTD events, indicating that DTD events likely originate from protofilament switching of individual motor heads.

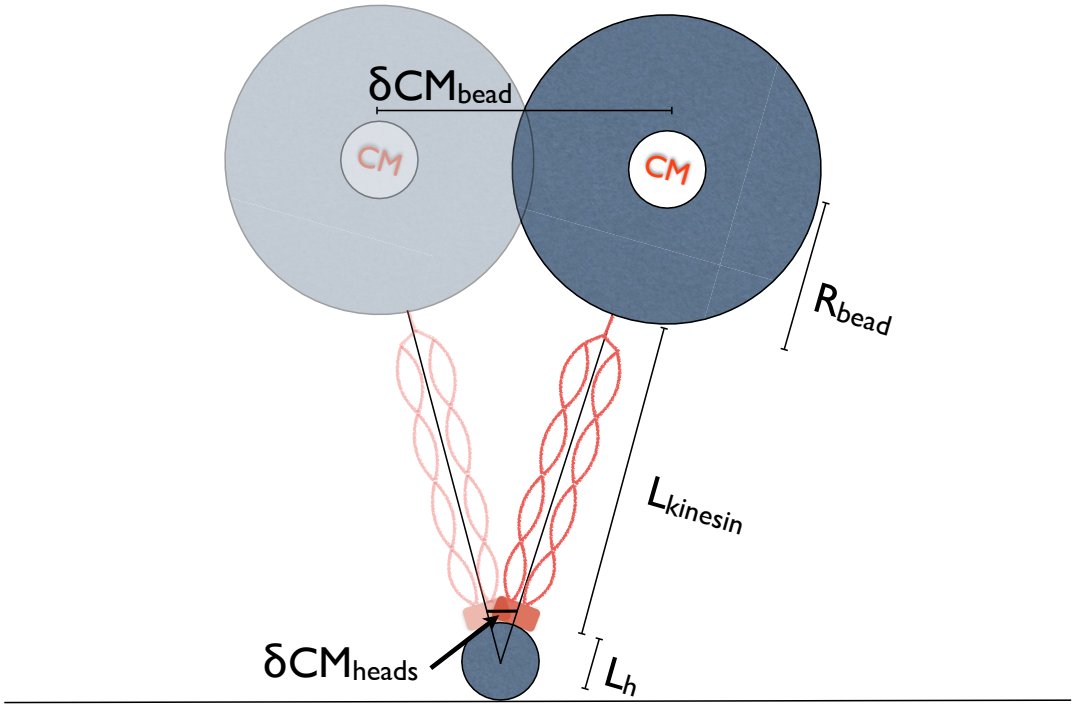

Supplementary Fig. 3: Geometrical projection of a change in bead center of mass (δCM_{bead} and its relation to a change in the kinesin motor head's center of mass (δCM_{heads}). Range of bead motion is given by constraints on the bead size, motor length, and microtubule dimensions. We find that $\delta CM_{heads} = \delta CM_{bead}(\frac{L_h}{R_{bead}+L_h+L_{kinesin}})$, with R_{bead} = bead radius, $L_{kinesin}$ = length of kinesin motors, and L_h = distance from center of microtubule to kinesin motor head's center of mass.

2 Attachment geometry

In the transverse direction there is more than an order of magnitude reduction in the standard deviation of transverse fluctuations for two-kinesin transport (around central peak) as compared to the standard deviation of transverse fluctuations of the single motor experiments (4.5 nm vs 55 nm respectively). This is much larger than the roughly 30% reduction as expected from a parallel suppression of fluctuations from both motors (i.e. motors in front and behind each other along the microtubule axis), assuming fluctuations are dominated by thermal motion. In the parallel case a 30% reduction in fluctuations would be due to the parallel addition of motor stiffness (spring constants) which results in an effective spring constant of twice the stiffness in the transverse direction, when both motors are in contact with the cargo and microtubule. Furthermore, fluctuations of the bead-cargo (transverse extension) would have the same thermal energy in the two and single motor cases, an energy which is proportional to the product of the effective spring constants and the square of the extensions (size of fluctuations). This implies that two motor transport with motors front and back to each other would have transverse fluctuations which have a magnitude of $2^{-1/2} \sim 0.7$ the magnitude of fluctuations with only one motor. A series suppression of fluctuations is physically unlikely (having motors attached head to tail) and would result in no reduction in transverse fluctuations, resulting in the only plausible scenario for the order of magnitude reduction be due to a geometric buttressing effect of having both motors being predominately side by side along the axis of the microtubule.

Buttressing the view that both motors are walking along the microtubule side by side and the assumption that fluctuations are thermal is an analysis of the axial fluctuations. In the axial direction there is approximately a 30% reduction in the magnitude of fluctuations for the two motor traces as compared to the single motor traces. This is equal to theoretical predictions for suppression of thermal motion with both motors acting in parallel against axial fluctuations of the bead due to both motors being predominately side by side.

Using the same attachment geometry as in Section 1, we applied trigonometry to a maximumly transverse displaced bead and calculated that the transverse angular rotation of the bead is limited to a total of approximately 87 degrees (Supplementary Fig. 1-2). (i.e. max angular extension $\sim 2\cos^{-1}(\frac{R_{bead}}{R_{bead}+L_{kinesin}+2R_{microtubule}})$). Through this 87 degree rotation of the center of mass of the bead the center of mass of the motor heads can only span up to 3 out of 13 protofilaments of the microtubule. The 9 peaks seen in the absolute transverse position histograms (Supplementary Fig. 6) are likely to be the result of the different locations the center of mass of the motor heads can take as the individual motor heads move across accessible protofilaments. A possible way in which the 4 motor heads could generate 9 peaks in the transverse position histogram can be seen in Supplementary Fig. 3.

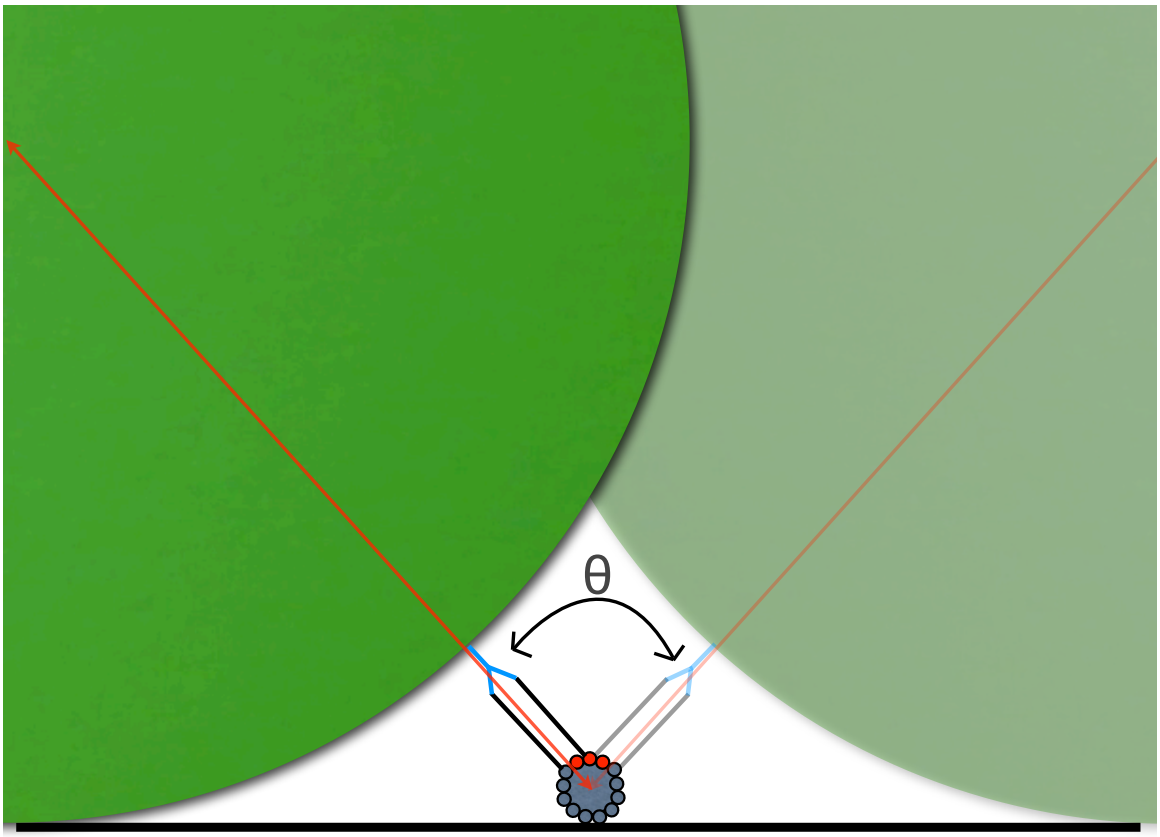

Supplementary Fig. 4: Bead cargo range of motion allowed in the transverse direction has a total angular play θ of 87 degrees with respect to the middle of the microtubule. Red arrows point from the center of the bead to the center of the microtubule and encompass approximately 3 protofilaments as the bead is displace maximumly in the transverse direction (these protofilaments highlighted in red). Figure drawn approximately to scale.

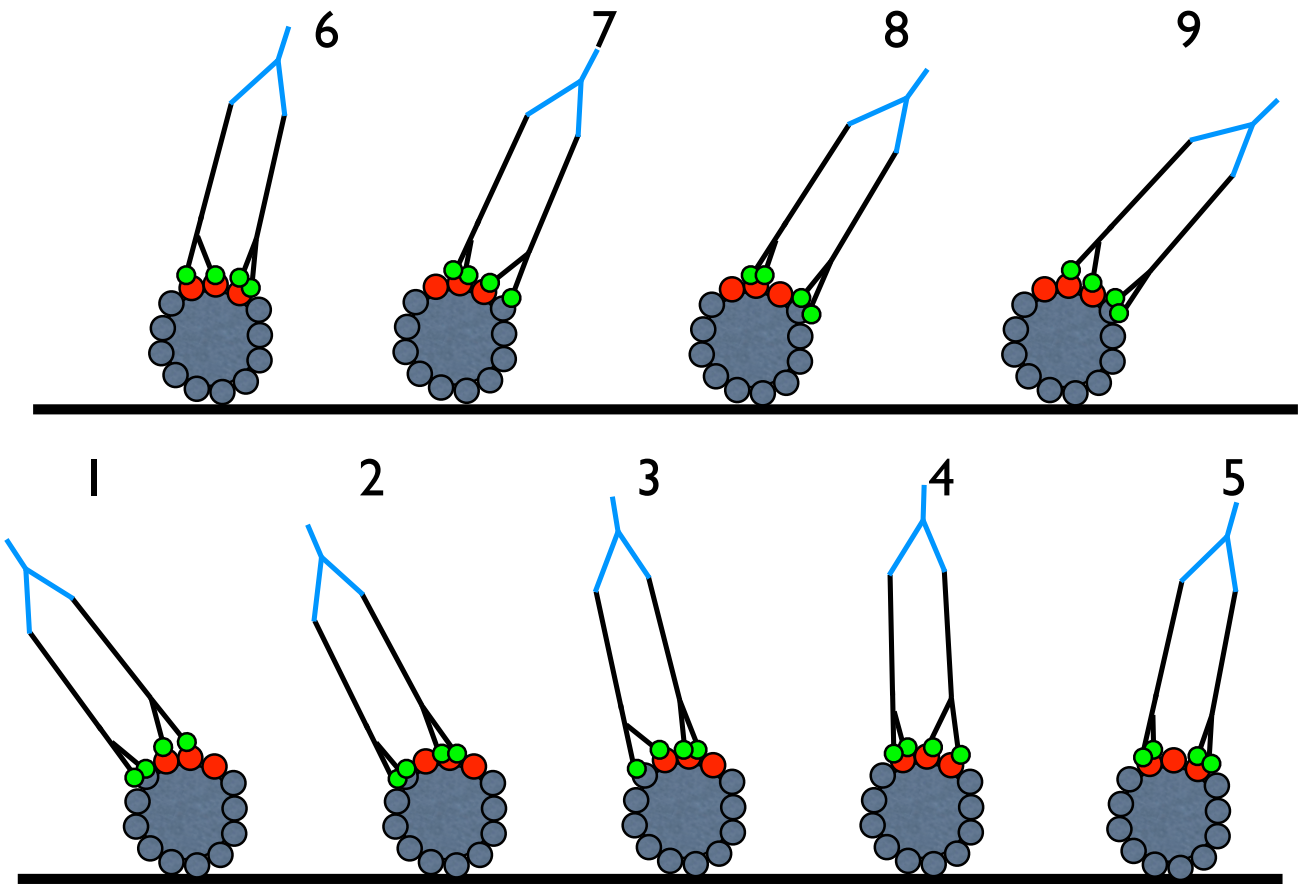

Supplementary Fig. 5: Nine example double motor head configurations across the three protofilament rotational degree of freedom (for motor head's center of mass) for the cargo-motor complex in the transverse direction.

3 Transverse motion at higher ATP concentrations

At 20 μM ATP the two motor traces appeared to also separate into two populations (Supplementary Fig. 7), although the high stepping rate compared to the observational frame rate introduced significant noise to observations. One group had histograms of transverse displacement which were very similar to the composite or average histogram of transverse displacement from traces at 10 μM ATP which had a greater than 5 μm travel distance. This group had frequent DTD events, high processivity with most traces leaving the 8 μm observation window, and a lower average velocity of 230 nm/s, while the non-DTD containing group at this ATP concentration had histograms of transverse displacement with high χ^2 differences from the composite histogram of transverse displacement of the DTD group at 10 μM ATP (Fig. 1), together with low processivity and higher travel velocities of 284 nm/s on average. This second group has the properties expected if the same physical phenomena responsible for the separation of traces at 10 μM ATP into two groups is also present and active at 20 μM ATP.

At the saturating (1 mM) ATP concentration of the kinesin motors, numerous steps are taken by the motors during each experimentally measured frame exposure (frame rate of 30/s), which would rule out the ability to observe DTD events at this concentration even though they may frequently occur during some traces at this ATP concentration. Nevertheless, since the overall histogram for processivity at this concentration is quite similar to the single motor case (Fig. 1A), we can tentatively conclude that if traces separated into DTD and non-DTD traces, similar to the 10 and 20 μM ATP traces, that both groups could be differentiated by their velocity and processivity (Supplementary Fig. 8). It may be possible that at the saturating ATP concentration that DTD events do not occur, a scenario which we are unable to rule out.

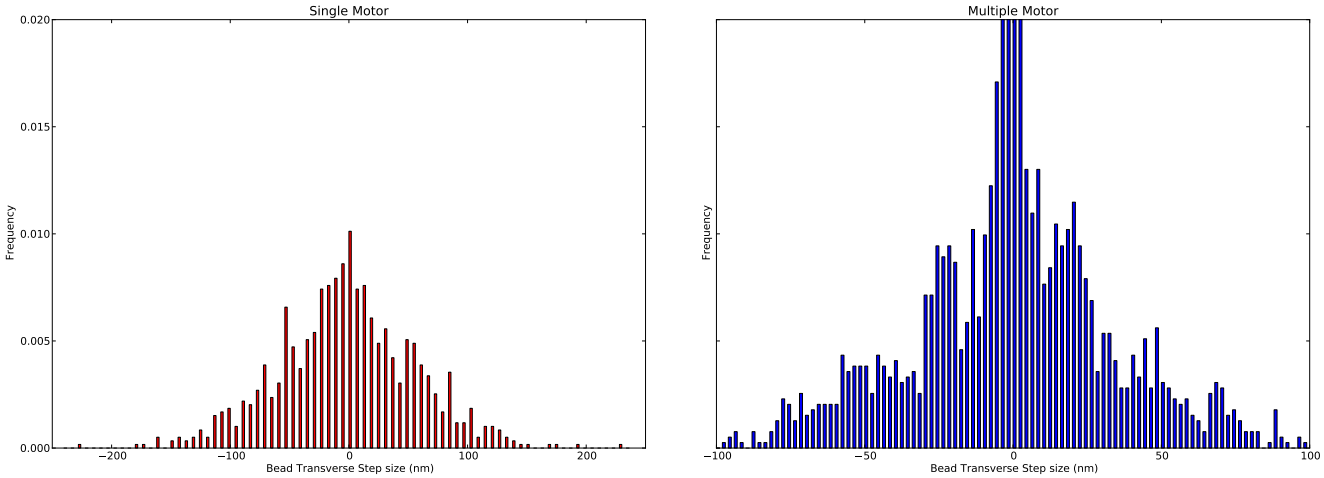

Supplementary Fig. 6: Histograms of transverse displacement for 200 nm beads at 20 μm ATP concentration. These transported bead-cargos, which have 45% of the diameter of the 440 nm beads used as cargo in our experiment, would result in transverse fluctuations which are approximately 41% smaller if the geometry is such as described by Equ. 1 in the geometry section above. In the two motor case (440 nm diameter beads) at an ATP concentration of 20 μM all transverse displacements have a standard deviation of 41.7 nm. The geometrical model we use in the paper would predict (Equ. 1) the standard deviation to reduce to approximately 24.7 nm if the bead size were reduced to 200 nm and experimentally we measured transverse fluctuations (200 nm diameter bead, multiple motors) to have a standard deviation of 23.4 nm, close to the predicted value.

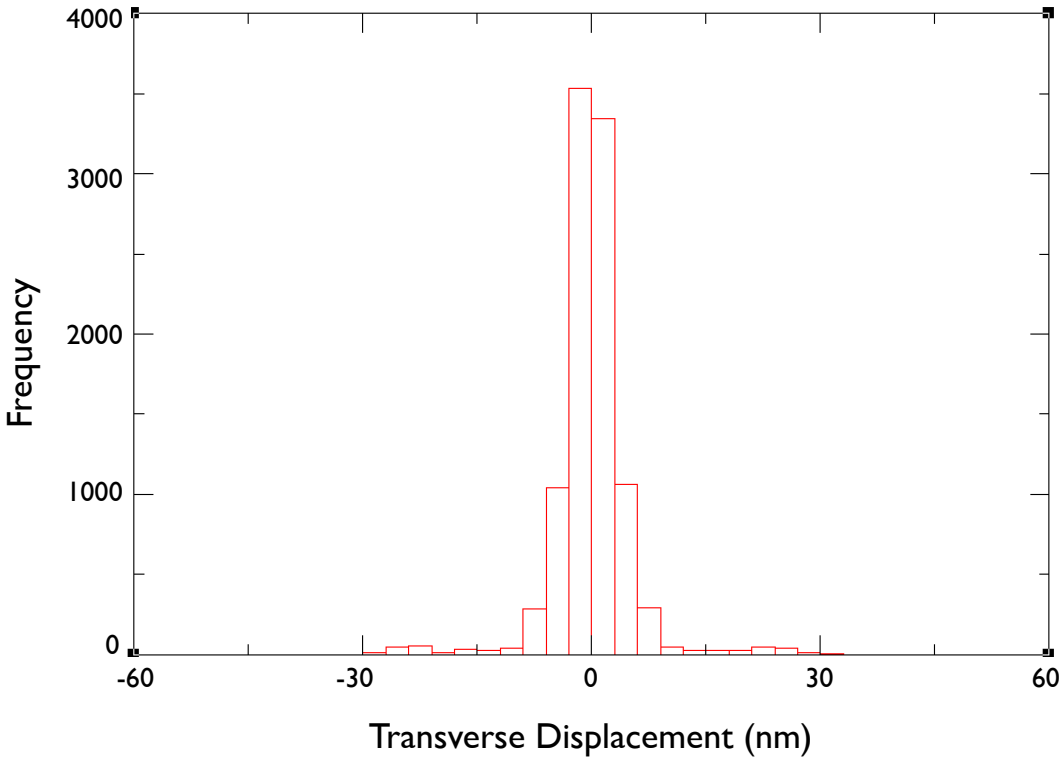

Supplementary Fig. 7: Histogram of transverse displacement for beads which have been fixed in position via chemical binding to a substrate. Positional noise is small, with a standard deviation of fixed bead displacement of 4.5 nm.

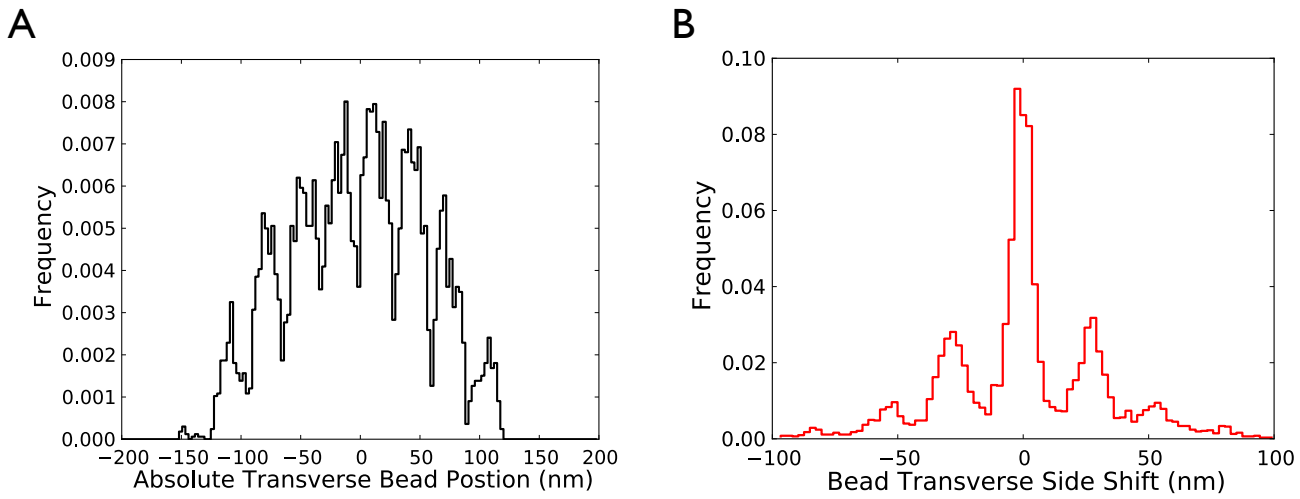

Supplementary Fig. 8: (A) A histogram of a particular trace's absolute bead center of mass transverse position. Given the nature of these histograms of absolute transverse cargo position we feel it is improbable that the presence of DTD events is due to the flexibility or conformational changes in the two motor construct itself given that DTDs result in preferred absolute positions for the center of mass of the bead. Traces show up to 9 distinct preferred positions or 'peaks' in the histogram of absolute transverse position of the cargo bead. Peaks in the absolute transverse position histogram are spaced by approximately 27 nm, close to the average transverse differential sidestep size measured. It is unlikely that there exists multiple conformational changes of the kinesin motors-linker complex which are of approximately the same magnitude, or that the changes in motor conformation affect the bead position identically to motors moving from protofilament to protofilament. Rather peaks in the absolute transverse position histogram likely correspond to different attachment geometries of the two kinesin motors to the microtubule surface (Supplementary Fig. 3). Furthermore, given the geometry of the two motor construct, each peak in the absolute transverse position histogram corresponds to the projection of a single motor head moving to an adjacent protofilament, and that DTD events which are 27 nm in size correspond to single motor heads moving to adjacent protofilaments. (B) Histogram of the differential step size in the transverse direction for this particular trace from part (A) which shows a low degree of noise such that seven peaks can be seen representing primary, secondary, and tertiary DTD events together with a central peak representing no motion.

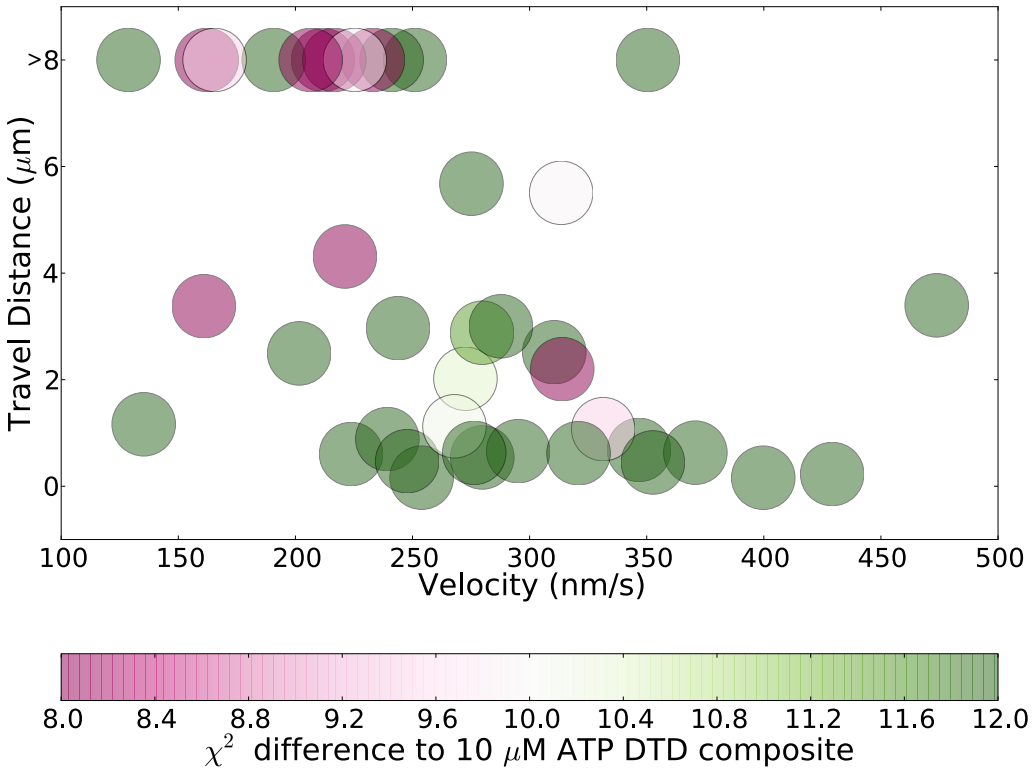

Supplementary Fig. 9: 20 μM ATP concentration two-kinesin transport traces separate broadly into two groups. One group has traces that have histograms of transverse displacement with low χ^2 difference to the composite histogram of transverse displacement of the DTD group at 10 μM ATP. This group is represented by pink circles, and has traces which tend to have high processivity, leave the 8 μm observation window, and have a velocity lower than traces which have high χ^2 differences to the composite histogram of transverse displacement of the DTD group at 10 μM ATP (in green). The non-DTD group traces at this 20 μM ATP concentration (green circles) tend to have a low processivity and have an average velocity of 284 nm/s as compared to the pink DTD group which has an average velocity of 230 nm/s.

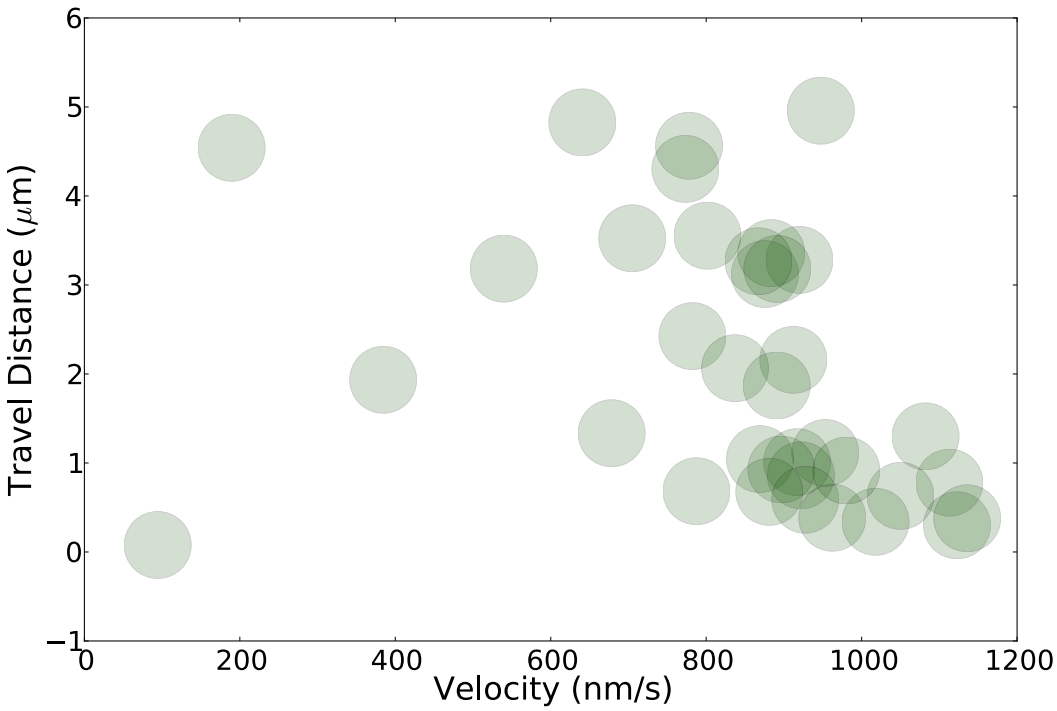

Supplementary Fig. 10: At 1 mM ATP concentration individual two-kinesin transport traces are plotted showing their processivity versus their velocity.

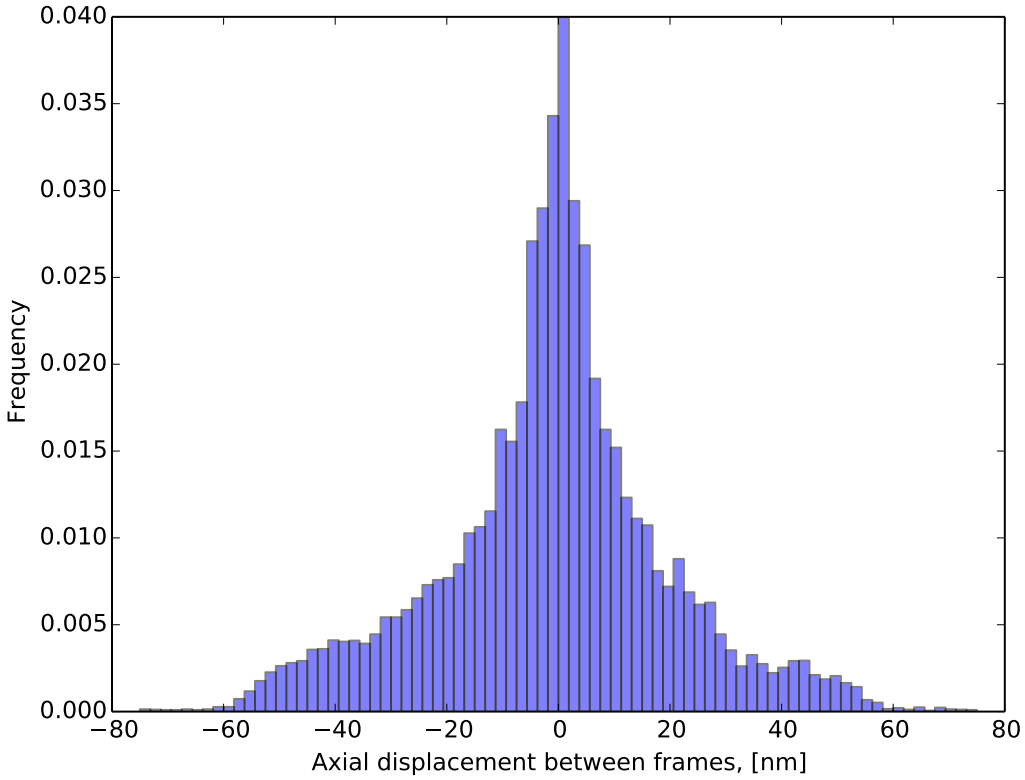

Supplementary Fig. 11: Histogram of axial movement between frames for traces which are longer than 8 μm.